

Birefringence and orientation of polyethylene zone-drawn under various thermomechanical conditions*

M. Hoff† and the late Z. Pelzbauer

*Institute of Macromolecular Chemistry, Czechoslovak Academy of Sciences,
Heyrovsky Sq. 2, 162 06 Prague 6, Czechoslovakia*

(Received 25 June 1991; revised 13 January 1992; accepted 11 February 1992)

In this paper, the influence of deformation and thermomechanical drawing conditions on the development of birefringence and orientation in high-density polyethylene during zone drawing is described. The orientation process of the crystalline phase does not proceed uniformly with deformation and is complete at lower draw ratios, while orientation of the amorphous phase increases continuously up to the highest draw ratios. The maximum birefringence considerably exceeds that of a polyethylene crystal (as high as 0.081) and the amorphous orientation almost approaches that of the crystalline phase. This indicates that the zone-drawing technique is highly effective in producing orientation. The birefringence is affected simultaneously by drawing stress and temperature; at higher temperatures and lower stresses, softening effects predominate, while in the opposite case stiffening effects become operative. The occurrence of both factors is regulated by the time of thermal exposure in the heating zone.

(Keywords: birefringence; orientation; polyethylene; zone drawing; deformation)

INTRODUCTION

During drawing of a semicrystalline polymer, its birefringence increases as a consequence of chain orientation in the direction of stress. The birefringence can be expressed in terms of the equation derived by Stein¹:

$$\Delta n = \Delta n_c + \Delta n_a + \Delta n_f + \Delta n_d \quad (1)$$

where $\Delta n_c = \Delta n_c^\circ f_c \alpha_c$ and $\Delta n_a = \Delta n_a^\circ f_a (1 - \alpha_c)$ are the birefringences of the crystalline and amorphous phases, respectively; Δn_c° and Δn_a° are the intrinsic birefringences of the crystalline and amorphous phases; f_c and f_a are the respective orientation factors; Δn_f and Δn_d are the form and deformation birefringences; and α_c is the percentage crystallinity.

The published values of the intrinsic phase birefringence of polyethylene²⁻¹¹ have been in the range of 0.048–0.0585 for Δn_c° and 0.042–0.261 for Δn_a° . The most frequently used values $\Delta n_c^\circ = 0.0585$ and $\Delta n_a^\circ = 0.2$ are employed for calculations in this study. The terms Δn_f and Δn_d will be neglected in the current calculations (it is true that Δn_f can make up 5–10% of the total birefringence but it will decrease considerably with the deformation ratio¹²). Then, according to equation (1), provided that values of Δn , α_c and f_c are known, the factor f_a can be estimated¹³.

The birefringence of polyethylene depends on the deformation ratio λ in a similar way for both tensile drawing (λ is the draw ratio) and extrusion (λ is the extrusion ratio)¹⁴⁻¹⁷. First, Δn increases very steeply up

to $\lambda \approx 5-10$, then it increases much more slowly. Depending on the deformation technique, the limiting value of Δn exceeds the intrinsic birefringence Δn_c° : when using drawing in an oven or solid-state extrusion, the highest value obtained has been 0.062^{14,15,17}; while using the zone-drawing technique, values as high as 0.065–0.076 have been reported^{11,18}. Crystal orientation increased quickly with the deformation ratio up to λ between 5 and 10, and f_c reached values very close to 1 for the parallel alignment of chains ($f_c = 0.97-1.0$)^{14,16,19,20}. Orientation of the amorphous phase increased monotonically over the whole range of λ . The factor f_a reached values of 0.2–0.8^{16,19,20}.

This study is to be a continuation of our previous papers on polyethylene treated by the zone-drawing technique with constant load²¹ and the resulting morphology²² and thermal shrinkage²³.

EXPERIMENTAL

The material used was blown, preoriented film ($\lambda_0 = 1.37 \pm 3.7 \times 10^{-2}$, $\Delta n_0 = 0.0028 \pm 8 \times 10^{-5}$) of linear polyethylene Liten VB33 (Chemical Works Litvinov, Czechoslovakia), which had a density of 0.958 g cm⁻³ and a molecular weight $\bar{M}_w = 197\,000$, $\bar{M}_n = 22\,000$.

The drawing method in non-isothermal (NR) and isothermal (IR) regimes has been described in detail elsewhere²¹. Here, it is essential to emphasize that the drawing temperature T_D was the temperature of the heating zone. After an initial stress σ_0 was applied (a load was hung on the sample), the polymer drew. Then, a true stress $\sigma = \sigma_0 S_0/S$ acts upon the narrowing neck, where S_0 and S are the cross-sections of the original and drawn samples. The draw ratios were determined as

* Dedicated to Dr Frantisek Hoff on the occasion of his 70th birthday

† Present address: University of Bristol, H. H. Wills Physics Laboratory, Tyndall Avenue, Bristol BS8 1TL, UK

$\lambda = \lambda_0 S_0/S$. Drawing was complete after sample fracture at a stress σ_F and a draw ratio λ_F .

When using the zone-drawing technique, the polymer passes through the heating zone with a certain velocity. Therefore, values of the zone temperature T_D and the real temperature of the sample may differ. This difference becomes more pronounced as the velocity increases with T_D and stress. Thus, the polymer can be drawn in the solid state even if T_D exceeds its melting point, depending on the stress²¹⁻²³. By choosing the appropriate values of T_D and σ_0 , drawing can be performed either in the solid state ($T_D < T_{0,m}$ or $T_D > T_{0,m}$ and $\sigma_0 > 3$ MPa) or in the melt ($T_D > T_{0,m}$ and $\sigma_0 < 3$ MPa)²². The value $T_{0,m} = 130-132^\circ\text{C}$ was the melting point of the undrawn polymer as determined from the disappearance of birefringence.

The birefringence was measured using a Reichert polarizing microscope equipped with a Berek compensator. The density of the polymer, ρ , was measured using the flotation technique in mixtures of CCl_4 and n-heptane. The samples were narrow strips with given draw ratios cut out from the neck²³. The volume crystallinity:

$$\alpha_c = (\rho - \rho_a)/(\rho_c - \rho_a) \quad (2)$$

was then calculated ($\rho_a = 0.854 \text{ g cm}^{-3}$ and $\rho_c = 0.9972 \text{ g cm}^{-3}$ are the densities of crystalline and amorphous polyethylene, respectively)²⁴.

RESULTS AND DISCUSSION

The experimental dependences of the birefringence as a function of the draw ratio are shown in *Figure 1*. For samples drawn in both IR and NR conditions, all curves have a steep region at the beginning of drawing and a subsequent slowly increasing region. Both regions can be regarded as linear and they intersect at the retardation point ($\lambda_r, \Delta n_r$). The increase in birefringence with draw ratio (the orientational efficiency) is then equal to the slopes of the respective parts of the curves before and after retardation, respectively:

$$v_1 = (\Delta n_r - \Delta n_0)/(\lambda_r - \lambda_0) \quad (3)$$

$$v_2 = (\Delta n_F - \Delta n_r)/(\lambda_F - \lambda_r) \quad (4)$$

where Δn_F is the birefringence at the place of fracture. The dependences of Δn_r , λ_r , v_1 , Δn_F and v_2 on the thermomechanical conditions of drawing are summarized in *Figure 2*.

Birefringence and draw ratio

For $\lambda < \lambda_r$. In agreement with data already published¹⁴⁻¹⁷, the steep increase in birefringence at $\lambda < \lambda_r$ can be attributed prevalently to orientation of the crystalline phase. At the retardation point on the curves $\Delta n = f(\lambda)$ in *Figure 1*, this process was completed and, at $\lambda > \lambda_r$, the crystallites can be considered as uniaxially oriented^{14,16,19,20}.

Figures 2a and *2b* show that in IR at $T_D = 104^\circ\text{C}$ both Δn_r and λ_r increase within the whole range of σ_0 used. At higher temperatures, there is a maximum; the higher T_D , the lower is σ_0 at the maximum. Above $T_{0,m}$, both quantities first decrease in the melt-drawing region until σ_0 reaches the value of 3 MPa for the transition into solid-state drawing. In NR, Δn_r and λ_r also decrease with σ_0 until drawing again takes place in the solid state.

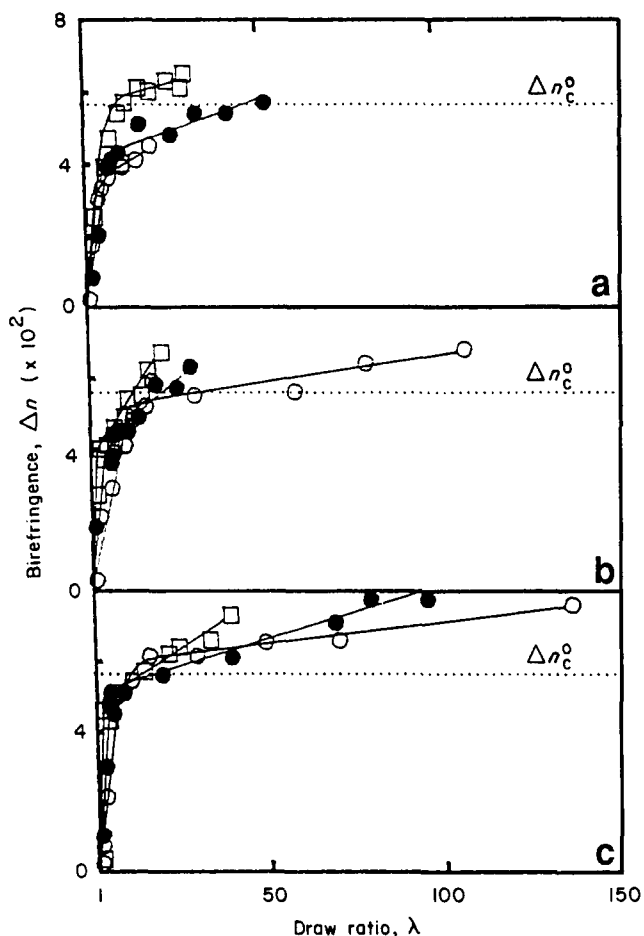


Figure 1 Birefringence of polyethylene, Δn , as a function of the draw ratio λ . Drawing carried out at: (a) IR, $T_D = 112.5^\circ\text{C}$, $\sigma_0 = 4$ (○), 7 (●), 15 MPa (□); (b) IR, $T_D = 138^\circ\text{C}$, $\sigma_0 = 0.8$ (○), 2.5 (●), 10 MPa (□); (c) NR, σ_0 (MPa), T_N ($^\circ\text{C}$) and T_F ($^\circ\text{C}$) are 0.8, 130.4 and 140.2 (○), 9, 72.9, 108.5 (●), and 13, 52, 101.6 (□). T_N and T_F are the temperatures of neck formation and fracture²¹; Δn_c^0 is the intrinsic crystalline birefringence of polyethylene

Then, the dependences pass through a maximum at $\sigma_0 \approx 8$ MPa. A linear relation was found between Δn_r and λ_r , irrespective of drawing conditions (regression function $\Delta n_r = 0.0385 + 0.0017\lambda_r$).

The orientational efficiency v_1 is inversely dependent on the drawing conditions (*Figure 2c*) as is evident from the linear relation $1/v_1$ versus λ_r , shown in *Figure 3*. This fact means that birefringence increases more slowly with λ if the crystalline orientation has been completed at higher draw ratio and vice versa.

The course of orientation of both the crystalline and the amorphous phase as well as the contributions of Δn_c and Δn_a to the total birefringence were judged from the λ_r values and equation (1). For $\lambda \geq \lambda_r$, the plateau value of $f_{c,sat} = 0.97$ was taken from ref. 20; f_a was calculated according to equation (1) assuming that the form and deformation birefringences were negligible.

The density was found to increase with λ_r and the melt-drawn samples had a higher density than those drawn in the solid state (*Figure 4a*).

As mentioned above, the factor f_c may be regarded as reaching its constant saturated value at λ_r . The fact that λ_r changes with T_D and σ_0 (*Figure 2b*) then means that, within the interval $1 < \lambda < \lambda_r$, the slope $\Delta f_c/\Delta \lambda$ must increase linearly with λ_r . Consequently, the process of crystalline orientation does not proceed affinely to deformation but is faster the lower λ_r .

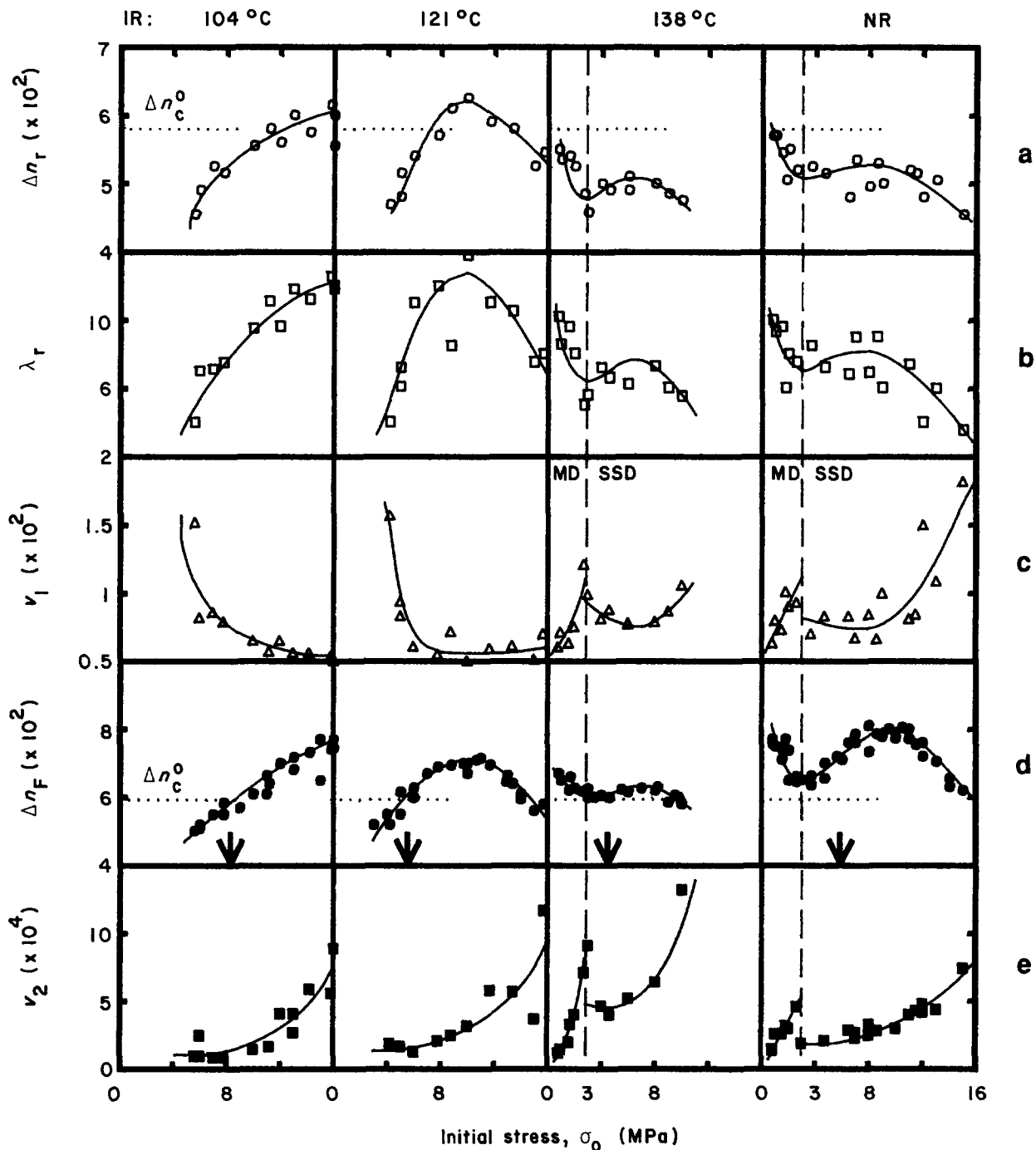


Figure 2 Birefringence behaviour of polyethylene drawn under various thermomechanical conditions. From top to bottom: (a) birefringence Δn_r , (b) draw ratio λ_r at the retardation point, (c) orientational efficiency v_1 before the retardation point, (d) birefringence at the place of fracture Δn_F , and (e) orientational efficiency v_2 after the retardation point, all versus the initial stress. Polymer drawn in IR at $T_D=104, 121, 138^\circ\text{C}$ and in NR; Δn_c^0 is the intrinsic crystalline birefringence; the vertical dashed line separates the melt-drawing (MD) and the solid-state-drawing (SSD) region; arrows denote the positions of the maxima of the draw ratio λ_F (ref. 21) on the σ_0 coordinate

The estimated orientation factor f_a increases linearly with λ_r (Figure 4b), so the increase in the amorphous orientation before the retardation point can be considered uniform with deformation ($df_a/d\lambda \approx 0.05$; calculated from the slope of the dependence $f_a = f(\lambda_r)$). As $f_c \gg f_a$ at the retardation point, the crystalline birefringence Δn_c contributes much more to the total value of Δn than the amorphous birefringence, Δn_a , as shown in Figure 4c. At the same time, Δn_a increases considerably faster with λ_r than Δn_c . This is due to a significant rise in f_a in the amorphous term in contrast to only a mild increase of α_c ($f_c = \text{constant}$) in the crystalline term in equation (1).

As to the density of the melt-drawn and the solid-state-

drawn polymer, there is evidently a difference between them (Figure 4a) but it is not great enough to affect the terms in equation (1) significantly. Consequently, the data points in Figures 4b and 4c for both melt- and solid-state-drawn polymers approximately fit single lines.

For $\lambda > \lambda_r$. An increase in birefringence with λ above λ_r is due to a further increase in the amorphous orientation and it is also somewhat influenced by the rise in crystallinity (Figure 5).

The ultimate birefringence at the place of fracture, Δn_F , usually exceeds the intrinsic crystalline birefringence (Figure 2d). In NR, being more favourable for high values

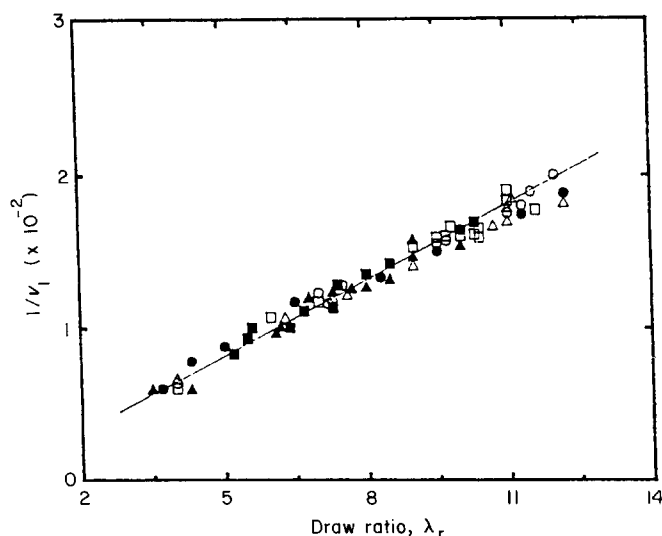


Figure 3 Linear relation between the reciprocal value of the orientational efficiency $1/v_1$ before the retardation point and the draw ratio λ_r at which orientation of the crystalline phase is completed. Polymer drawn in IR at $T_D=104$ (○), 112.5 (□), 121 (△), 129.5 (●), 138°C (◻) and in NR (▲)

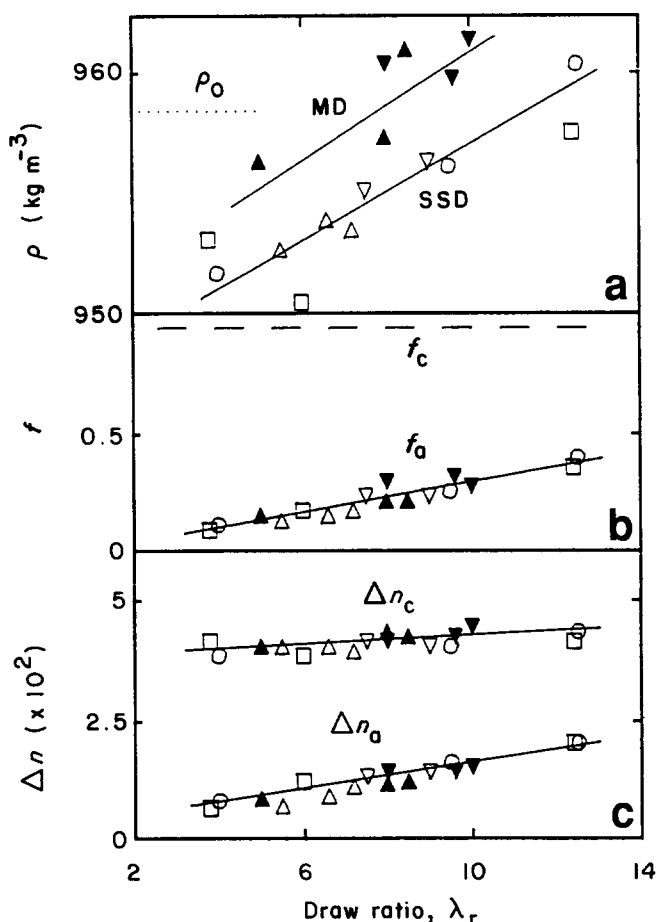


Figure 4 (a) Density ρ , (b) orientational factor f and (c) the crystalline and amorphous contributions to the total birefringence Δn as a function of the draw ratio λ_r at the retardation point. Polymer drawn in IR at $T_D=104$ (○), 129.5 (□), 138°C (in the melt (▲) and in the solid state (△)) and in NR in the melt (▼) and in the solid state (▽); ρ_0 is the density of the undrawn foil; the subscripts c and a denote the crystalline and amorphous phases, respectively

of Δn to be achieved, we obtained $\Delta n_F = 0.081$ with the sample drawn to $\lambda_F = 102$ at $\sigma_0 = 8$ MPa. This shows the high orientational effectiveness of the drawing method employed.

The shape of the curves $\Delta n_F = f(\sigma_0)$ (Figure 2d) is very similar to that for Δn_r (Figure 2a). Hence, the birefringence behaviour of the polymer above λ_r is pre-determined by the state immediately after the completion of the crystalline orientation. The orientational efficiency v_2 in this stage of drawing increases with σ_0 and somewhat with T_D as well (Figure 2e). The passage from the melt-drawing to the solid-state-drawing region is accompanied by a drop on the curve $v_2 = f(\sigma_0)$; the orientational efficiency has decreased because of the presence of a solid state.

A mild increase of α_c after the retardation point (by only about 6% when $\lambda_F - \lambda_r \approx 90$) only slightly affects the crystalline term Δn_c of equation (1), so the extreme values of Δn_F must be accompanied by high values of the factor f_a . Its estimate, along with those of Δn_c and Δn_a , are illustrated for highly drawn samples in Table 1 (the prerequisites necessary for the calculations have been quoted above). Under proper drawing conditions, f_a can reach values compared with those of f_c .

Table 1 Estimations of the amorphous orientation factors f_a and the crystalline (Δn_c) and the amorphous (Δn_a) contributions to the total birefringence Δn_F at the place of polymer fracture. λ_F and ρ are the respective draw ratios and densities

Regime	T_D (°C)	σ_0 (MPa)	λ_F	ρ (g cm ⁻³)	Δn_F	f_a	Δn_c	Δn_a
IR	104	16	35	0.9662	0.078	0.77	0.044	0.034
	112.5	13	34	0.9645	0.070	0.57	0.044	0.026
	121	10	41	0.9650	0.071	0.60	0.044	0.027
	129.5	7	52	0.9683	0.068	0.56	0.045	0.023
	138	0.7	110	0.9788	0.068	0.70	0.049	0.019
NR	141.1	0.8	144	0.9762	0.077	0.97	0.048	0.029
	117.2	8	102	0.9684	0.081	0.89	0.045	0.036

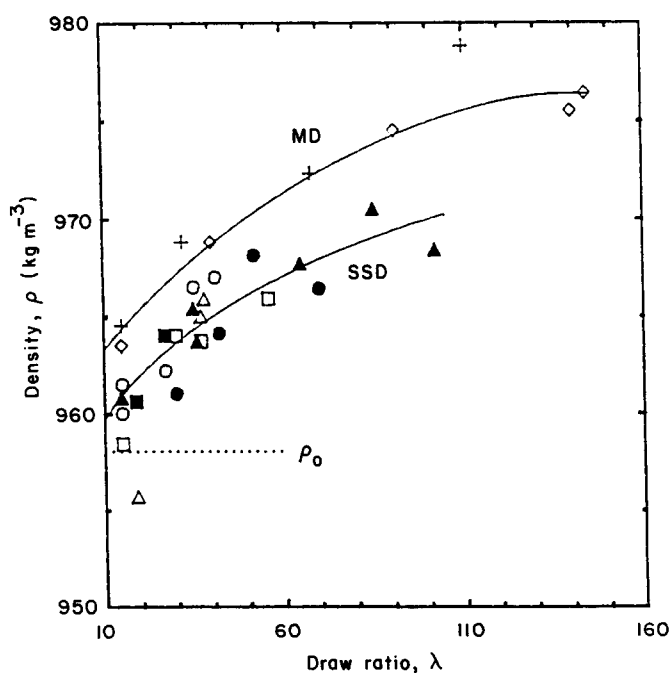


Figure 5 Effect of the draw ratio λ on the density ρ after the retardation point with solid-state drawing (SSD) and melt drawing (MD). Polymer drawn in IR at $T_D=104$ (○), 112.5 (□), 121 (△), 129.5 (●), 138°C (in the melt (+) and in the solid state (■)) and in NR in the melt (◇) and in the solid state (▲); ρ_0 is the density of the undrawn foil

Birefringence and thermomechanical conditions of drawing

The orientational efficiency of drawing is affected by the time of thermal exposure in the heating zone, t_{exp} , which, in turn, can be controlled by choosing the proper T_D and σ_0 . The higher the values of T_D and σ_0 , the faster the polymer flows through the zone (shorter t_{exp}) and vice versa²⁵. Structural changes are not compelled by a constant cross-head speed as in a tensile tester, but rather the changes themselves regulate the strain rate. Therefore, at a given T_D and σ_0 , softening and stiffening lead to an optimum orientation. Such self-regulation in drawing gives a structure with an almost unperturbed, adequately stretched molecular network, as has been proved by the high thermal shrinkage of drawn samples²³.

For $\lambda < \lambda_r$. As has been shown above, the process of crystalline orientation is decisive for the orientational efficiency v_1 (Figure 2c). To make polymer crystals deform plastically, the physical bonds among chains in a crystal lattice must be broken by either a stress or a rise in temperature or by both. Furthermore, to initiate chain slip, a certain induction period t_{ind} is needed. This will decrease with increasing temperature and stress²¹. As the drawing temperature was chosen above the crystalline relaxation dispersion temperature $T_{\alpha(c)}$ (except NR, where T_D drops below this value at higher σ_0), which is 70–90°C for polyethylene, a portion of less perfect crystals can melt and accelerate the process of crystalline orientation by crystallization in a stretched conformation, or by acting as a plasticizer. A partial melting has been proved by our previous findings²². Obviously, this effect becomes more pronounced at higher temperatures and longer thermal exposures.

In the IR solid-state-drawing region at low initial stresses, the polymer flows through the heating zone slowly and t_{exp} is long enough so that the thermal softening effects become prevalent. This enables significant orientational efficiency v_1 (Figure 2c). With rising σ_0 , the polymer flow through the heating zone becomes faster and t_{exp} shorter, restricting the thermal effects. The value of v_1 decreases as the true stress σ is still low and does not contribute to a disturbance of the crystalline lattice and, at the same time, $t_{ind} > t_{exp}$. After passing beyond a certain σ_0 value (corresponding to the v_1 minimum), the true stress is already sufficient to reorganize the crystalline phase and, moreover, $t_{ind} < t_{exp}$ so the orientational efficiency begins to increase. At a higher T_D , a lower stress is needed for intracrystalline chain slip and the v_1 minimum is shifted to lower σ_0 values. At $T_D = 104^\circ\text{C}$, this minimum lies beyond the range of the initial stress used.

In NR, the time of thermal exposure does not change very much, since a rise in σ_0 is compensated by a respective drop in the necking temperature, T_N (ref. 21). A balance between the thermal- and stress-softening effects is then controlled not by shortening t_{exp} at constant temperature but by a drop in temperature at a comparable t_{exp} . When the drawing temperature has passed below the α -crystalline relaxation region (at $\sigma_0 \approx 6\text{--}8\text{ MPa}$), the thermal-softening effects can be neglected and the reorganization of the crystals becomes exclusively a stress-controlled process. Then, as a consequence of the increasing true stress, v_1 goes up. These considerations are corroborated by the results of Sadler and Barham²⁶, who did not observe any melting effects during drawing of polyethylene below $T \approx 70\text{--}90^\circ\text{C}$.

In the melt-drawing region, the orientational efficiency is determined by the rate of extension of the molten chains before crystallization outside the heating zone; higher stresses are more favourable²². Moreover, the faster the polymer flows through the zone, the less the possibility of a partial relaxation of the molten chains and their subsequent refolding. A decrease of t_{exp} improves the conditions for crystallization in the oriented state. So, the orientational efficiency v_1 increases with σ_0 until $\sigma_0 > 3\text{ MPa}$, when drawing again takes place in the solid state (Figure 2c).

For $\lambda > \lambda_r$. The orientational efficiency v_2 increases with the initial stress (Figure 2e). Consequently, a sample drawn at a given T_D to a comparable λ is more oriented when a higher σ_0 has been applied, since the true stress is higher as well (Figure 6). This means that, at a given draw ratio, the amorphous orientation is influenced by the acting true stress at which the respective draw ratio was obtained.

The drop in v_2 compared with v_1 (ca. 10 times) along with the simultaneous increase in the true stress ($\sigma < 140\text{ MPa}$ at $\lambda < \lambda_r$ and $\sigma \approx 140\text{--}600\text{ MPa}$ at $\lambda_r < \lambda < \lambda_F$)²¹ shows that an increase in the amorphous orientation after the crystalline orientation has been completed is much more energy-consuming than the lamellar-to-fibrillar structural transformation. A rise in temperature facilitates the process; chain mobility increases and mutual adhesion among microfibrils during

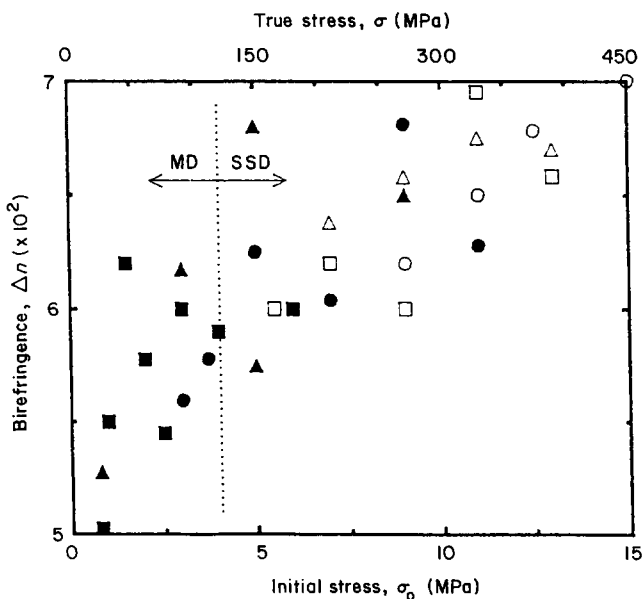


Figure 6 Plot of Δn versus σ_0 illustrating the increase of birefringence with the true stress $\sigma = \sigma_0$ at a given draw ratio ($\lambda = 30$). Polyethylene drawn in IR at $T_D = 104^\circ\text{C}$ (○), 112.5°C (□), 121°C (△), 129.5°C (●) and 138°C (■) and in NR (▲); MD (SSD) denotes the melt-drawing (solid-state-drawing) region

Table 2 Increase in the orientational efficiency of drawing v_2 after the retardation point with increasing drawing temperature T_D (IR). $\sigma_0 = 10\text{ MPa}$

T_D ($^\circ\text{C}$)	104	112.5	121	129.5	138
$v_2 \times 10^2$	0.020	0.028	0.031	0.036	0.13

their slip is reduced, which improves the extension of amorphous chains (Table 2). The difference between the melt drawing and solid-state drawing can be explained by an easy extension of chains in the melt before their crystallization and by an increase of the adhesion among microfibrils in the solid state.

In agreement with the above findings, the highest values of Δn_F were obtained in NR, which also gives the highest draw ratios²¹ and where drawing at comparable σ_0 values takes place at the highest true stresses. In the previous study²¹ we have shown the maxima of σ_F (analogous to the strength) to be shifted, compared with the maxima of λ_F , towards higher values of σ_0 . The maxima of Δn_F are shifted in a similar way. Hence, one can expect that an increase in the amorphous orientation brings an improvement in the mechanical properties of the polymer rather than an increase of the draw ratio itself.

CONCLUSIONS

The total birefringence increases linearly with the draw ratio in two different regions; first, steeply during orientation of the crystalline phase and then, after completing it, much more slowly.

The development of the crystalline orientation does not proceed affinely with deformation and is affected by the thermomechanical conditions of drawing. Simultaneous softening and stiffening effects are regulated by the time of thermal exposure of the polymer in the heating zone.

The amorphous orientation increases continuously during drawing up to the highest draw ratios. At the optimum drawing conditions Δn reaches values as much as 30% higher than the intrinsic birefringence of a polyethylene crystal. This is a consequence of the very high amorphous orientation. It gives evidence for the high orientational effectiveness of the zone-drawing technique.

The degree of amorphous orientation is not only a function of the draw ratio but it increases with the true stress at which the given draw ratio has been obtained.

ACKNOWLEDGEMENTS

M. Hoff wishes to thank Dr D. P. Heberer from the University of Bristol for helping in preparing the manuscript and the late Dr Z. Pelzbauer for everything he had been allowed to learn from him.

REFERENCES

- 1 Stein, R. S. *J. Polym. Sci.* 1958, **31**, 327
- 2 Denbigh, K. G. *Trans. Faraday Soc.* 1940, **36**, 939
- 3 Bunn, C. W. and de Daubenny, R. *Trans. Faraday Soc.* 1954, **50**, 1173
- 4 Stein, R. S. and Norris, F. H. *J. Polym. Sci.* 1956, **21**, 381
- 5 Gent, A. N. and Vickroy, V. V. *J. Polym. Sci. (A-2)* 1967, **5**, 47
- 6 Saunders, D. W., Lightfoot, D. R. and Parsons, D. A. *J. Polym. Sci. (A-2)* 1968, **6**, 1183
- 7 Desper, C. R., Southern, J. H., Ulrich, R. D. and Porter, R. S. *J. Appl. Phys.* 1970, **41**, 4284
- 8 Fukui, Y., Asada, T. and Onogi, S. *Polym. J.* 1972, **3**, 100
- 9 Nakayama, K. and Kanetsuna, H. *J. Mater. Sci.* 1975, **10**, 1105
- 10 Wedgewood, A. R. and Seferis, J. C. *Polym. Eng. Sci.* 1984, **24**, 328
- 11 Takahashi, T., Tanaka, T., Kamei, R., Okui, N., Takahiro, M., Umamoto, S. and Sakai, T. *Kobunshi Ronbunshu* 1988, **45**, 213
- 12 Rossignol, J. M., Seguela, R., Rietsch, F. and Dupuis-Lallemant, J. *J. Polym. Sci. (C)* 1989, **27**, 527
- 13 Stein, R. S. in 'Newer Methods in Polymer Characterisation', Wiley-Interscience, New York, 1964, Ch. 4
- 14 Mead, W. T., Desper, C. R. and Porter, R. S. *J. Polym. Sci., Polym. Phys. Edn.* 1979, **17**, 859
- 15 Capaccio, G., Gibson, A. G. and Ward, I. M. in 'Ultra-High Modulus Polymers' (Eds. A. Ciferri and I. M. Ward), Applied Science, London, 1979, Ch. 1
- 16 Kaito, A., Nakayama, K. and Kanetsuna, H. *J. Appl. Polym. Sci.* 1985, **30**, 1241
- 17 Kanamoto, T., Sherman, E. S. and Porter, R. S. *Polym. J.* 1979, **11**, 497
- 18 Kunugi, T., Oomori, S. and Mikami, S. *Polymer* 1988, **29**, 814
- 19 Seguela, R. and Rietsch, F. *Polymer* 1986, **27**, 532
- 20 Kaito, A., Nakayama, K. and Kanetsuna, H. *J. Macromol. Sci.-Phys. (B)* 1987, **26**, 281
- 21 Pelzbauer, Z. and Hoff, M. *J. Macromol. Sci.-Phys. (B)* 1990, **29**, 221
- 22 Hoff, M. and Pelzbauer, Z. *Polymer* 1991, **32**, 999
- 23 Hoff, M. and Pelzbauer, Z. *Polymer* 1991, **32**, 3317
- 24 Wunderlich, B. 'Macromolecular Physics', Academic Press, New York, 1973, Vol. I, pp. 97, 388
- 25 Hoff, M. in preparation
- 26 Sadler, D. M. and Barham, P. J. *Polymer* 1990, **31**, 36